Available online at www.sciencedirect.com
ScienceDirect
Tetrahedron 63 (2007) 7326–7333
Tetrahedron

Pyridine-containing versatile gelators for post-modification of gel tissues toward construction of novel porphyrin nanotubes

Sudip Malik,[a] Shin-ichiro Kawano,[a] Norifumi Fujita[a] and Seiji Shinkai[a,b,*]

[a]*Department of Chemistry and Biochemistry, Graduate School of Engineering, Kyushu University, Moto-oka 744, Nishi-ku, Fukuoka 819-0395, Japan*
[b]*Center for Future Chemistry, Kyushu University, Moto-oka 744, Nishi-ku, Fukuoka 819-0395, Japan*

Received 22 January 2007; revised 10 April 2007; accepted 4 May 2007
Available online 22 May 2007

Abstract—Low molecular weight gelators have recently been used as a template to construct novel kind of composite materials of different shape or structures such as helix, fibers, tape or tube through the electrostatic interaction between gelators and the intermediate molecules. In this article, we intricately apply the non-electrostatic interaction between gelator and fluorescent molecules to fabricate the gel fibers. To achieve our goal, we have intentionally designed pyridine containing cholesterol-based gelators **1**–**3** by keeping one thing in our mind that during the formation of the stacking column the pyridine moieties will be arranged like a spiral staircase around the cholesterol column. The gelation properties of these three gelators are tested in different solvents including sublimable solvents like naphthalene and the gelator **1** has emerged as a 'supergelator'. The morphologies strongly depend on the process of solvent removal from the gel state and the stabilities of gel have been tuned by the added metal ions like Ag(I) by using metal–ligand interaction. Lastly, we have decorated the gel fibers obtained from gelator **1** with fluorescent molecules like tetraphenyl porphyrin Zn(II) [**4**·**H** and **4**·**Zn**] having photopolymerizable unit at the end of tether groups and the modified fibers are well characterized by UV–vis absorption spectroscopy, confocal laser scanning microscopy as well as transmission electron microscopy. This is a novel example of decoration of gel fibers with fluorescent molecules and the process will offer an alternate application in photochemical and electrochemical devices.

1. Introduction

Low molecular-weight gels can be defined as thermally reversible and viscoelastic semi-solid materials that are generally composed of relatively low molecular-weight molecules at low concentrations in organic solvents or water.[1] In the gel phase, the low molecular-weight gelators give well-defined one-dimensional assemblies with a high structural aspect ratio, the images of which can be easily obtained by microscopic observations. Numerous examples have been reported on the different aspects of low molecular-weight gels, which are conventionally prepared by heating mixtures of gelator and solvent until the gelator dissolves; upon cooling the sol transforms to the gel. As a consequence of their intriguing properties, low molecular-weight gelators have got potential applications in various fields like plastic surgery,[2] cosmetics,[3] contact lenses,[4] solar cells,[5] sensorics,[6] light harvesting materials,[7] as well as being potential nanomaterials for opto- and electrical nanodevices. The gelation ability of such organogelators is often evaluated by three different factors: (1) the critical gelation concentration (CGC) where the sol phase changes into the gel phase, (2) the gel–sol phase transition temperature (T_{gel}), and (3) the gelation versatility for various solvents. Property (1) has frequently been reported and several 'supergelators', which can gelate the solvents at less than 1 wt % have been reported.[8] Property (2) has also been studied and 'thermally-stable gelators', which have T_{gel} values higher than their solvent boiling points have been reported.[9] On the other hand, property (3) has been generally less developed and in fact, there is no systematic guideline for the design of such gelators. In this paper, we have made a new approach to property (3) using pyridine-containing cholesterols. It is known that pyridine shows versatile solubility in both polar and apolar solvents (including water and cyclohexane). This suggests that the pyridine moiety in gelators may play a role in maintaining their affinity with

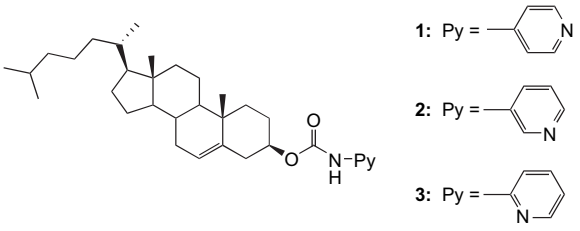

Figure 1. Chemical structure of compounds **1**–**3**.

* Corresponding author. Tel.: +81 92 802 2824; fax: +81 92 802 2820; e-mail: seijitcm@mbox.nc.kyushu-u.ac.jp

0040–4020/$ - see front matter © 2007 Elsevier Ltd. All rights reserved.
doi:10.1016/j.tet.2007.05.027

Table 1. Gelation properties of compounds **1–3** at rt[a]

Solvent	State[b]		
	1	**2**	**3**
n-Hexane	G	P	PG
Cyclohexane	G	S	PG
n-Octane	G	P	PG
Benzene	G[e]	S	S
Toluene	G[d]	PG	S
p-Xylene	G	S	S
THF	S	S	S
Anisole	G	G	S
Diphenyl ether	G[c]	S	G
Methanol	G[c]	P	PG
Ethanol	G[d]	P	PG
1-Butanol	G[d]	S	PG
Ethylacetate	G	P	PG
Acetone	G	P	PG
CH_3CN	G[c]	P	PG
$CHCl_3$	S	S	S
DMF	G[d]	S	PG
DMSO	G[d]	P	G
H_2O	I	I	I

[a] Concentration of the compound is 19.7 mol dm^{-3} (1.0 wt %).
[b] G: gel, PG: partial gel, P: precipitation, S: solution, I: insoluble when heated.
[c] Gel at 0.5 wt %.
[d] Gel at 2.5 wt %.
[e] Gel at 3.5 wt %.

solvent molecules. With this idea in mind, we designed pyridine-containing cholesterol-based gelators **1–3** (Fig. 1), hoping they would exhibit versatile gelation ability for many organic solvents.

2. Results and discussion

Compounds **1** (mp 192–193 °C), **2** (mp 211–214 °C), and **3** (mp 199–200 °C) were synthesized by the reaction of cholesteryl chloroformate with the corresponding aminopyridine in the presence of triethylamine and identified by ^{1}H NMR and MALDI-TOF mass spectral evidence and elemental analyses.[10]

The gelation ability of **1–3** was tested for 19 different solvents with 10 g dm^{-3} (19.7 mmol dm^{-3}) as a standard concentration. The results are summarized in Table 1. Compound **2** shows eight 'S' marks (soluble at 10 g dm^{-3}) and eight 'P' marks (soluble at reflux temperature but precipitate at 25 °C). Hence, it is either too soluble or too crystalline. Compound **3** makes 12 solvents gelatinous, but 10 solvents among them gel only partially, as shown with 'PG'. Presumably, **3** tends to form microcrystalline particles. On the other hand, compound **1** can gel 10 solvents at 10 g dm^{-3}, 15 solvents at 25 g dm^{-3}, and 16 solvents at 35 g dm^{-3}. These results clearly support the view that **1** is a unique gelator possessing property (3). With respect to 'property (1)', methanol, acetonitrile, and diphenyl ether gel even at 5.0 g dm^{-3}, indicating that **1** has the character of a 'supergelator'. The T_{gel} values determined at 10 g dm^{-3} in diphenyl ether were 100 °C for **1** and 67 °C for **3**. The results indicate that **1** also has property (2).

It is not yet clear what the origin of the difference between **1** and the others is. The cholesterol moieties may be provided to form a one-dimensional stacking column, the pyridine moieties will be helically arranged, like a spiral staircase, around the cholesterol column (Fig. 2, left). Pyridine has a dipole running from 4-C to 1-N. In the one-dimensional columnar aggregate of **1**, therefore, the dipoles are arranged in a radial fashion around the central cholesterol column. This aggregation mode may be effective to maintain the gel stability and to suppress the undesired further coagulation. As expected, a well-developed network structure composed of fine fibrils was observed in the transmission electron microscopy (TEM) picture (Fig. 2, right).

It is interesting that these versatile gelators can be applied to a sublimable solid solvent, which has shown efficiencies to prepare multiporous materials with polymers.[11] Naphthalene is a well-known sublimable substance, which is a solid at room temperature. Upon heating, naphthalene melts and turns to a liquid at 83 °C. We added the gelator (**1** or **3**) (30 wt %) to naphthalene in sealed-cap vials and heated until the mixtures dissolved. After homogeneous solutions were obtained, the samples were cooled to room temperature and the melting points of the solid masses thus obtained were then evaluated. Although the solid mass prepared from **1** did not have a clear melting point upon heating, it was noteworthy that the solid mass prepared from **3** melted at around 130 °C (cf. **3**: mp 198 °C), which was 47 °C higher than melting point of naphthalene. These observations indicate that the gel fibers are homogeneously dispersed in the solid mass and exert a strong effect on the melting point. Some sublimable substances such as naphthalene and *p*-dichlorobenzene are known to have insecticidal properties. The above finding implies that it is possible to tune the sublimation speed by preparing composites with certain concentration of the gelator.

To obtain visual images of the assembled gelators in naphthalene, we analyzed the samples by scanning electron microscopies (SEM). For the SEM observation, a carbon-

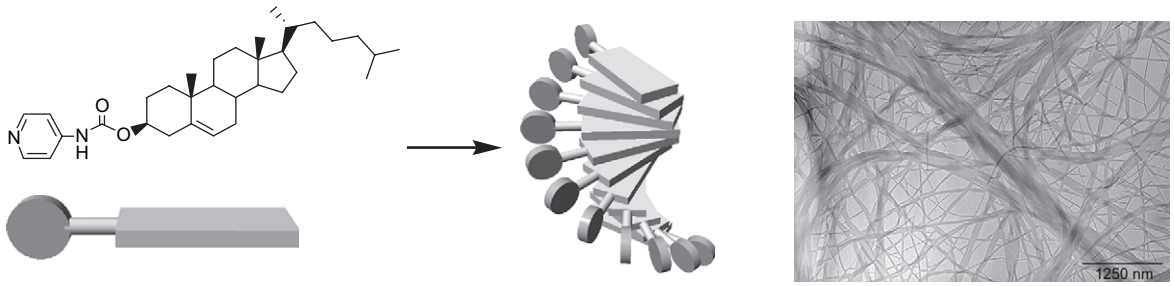

Figure 2. Schematic representation of the assembling mode of **1** and TEM image of the *p*-xylene gel of **1** (10 g dm^{-3}).

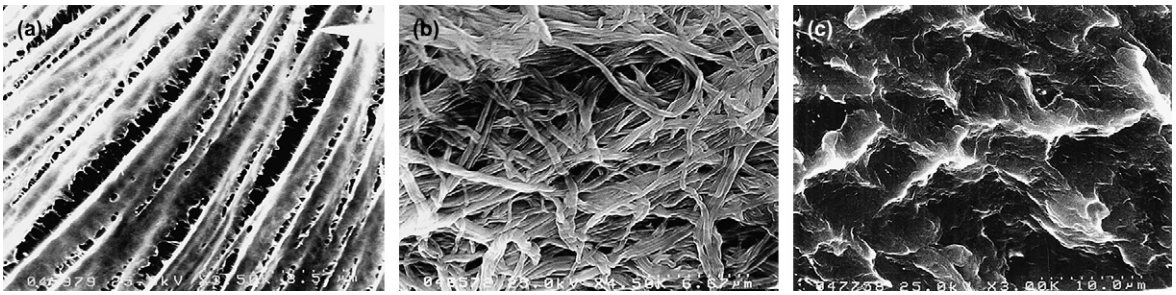

Figure 3. SEM pictures of xerogel of **1** prepared from (a) naphthalene and (b) benzene, and (c) freeze-dried sample prepared from benzene solution of **1**.

coated copper grid was immersed in the hot solution of the mixture and cooled at room temperature. After cooling, the naphthalene in the sample was thoroughly removed under vacuum condition in a desiccator for 10 days. The complete removal of naphthalene from the composite with the gelator was confirmed by UV–vis spectral analyses (data not shown). As seen in Figure 3a, unprecedented whisker-like morphologies have been observed from the sample prepared from the **1**/naphthalene mixed system. In the case of conventional organic solvents (benzene, toluene, xylene, etc.) we always observed a fibrillar type morphology from the xerogel of **1** (Fig. 3b). If we freeze-dry the gel of **1** prepared from the benzene gel, i.e., removing the solvent in the solid state, the morphology is surprisingly altered to a sheet-like structure (Fig. 3c). The results indicate that the morphology of **1** strongly depends on the solvent and sample preparation, and the whiskers are observed only for the sublimable solvents with **1**.

Recently, low molecular-weight gels (LMWGs) have been used as templates or molds to create various kinds of composite materials. This approach has received great attention because LMWGs provide various hierarchical nanostructures such as helix, fiber, tape, tube, sheet, etc. and such nanostructures can be readily transcribed to the other material sources such as inorganic compounds and polymer materials (Table 2, top). In this context, we and others have explored the new method to transcribe a variety of organic superstructures into inorganic materials by sol–gel reaction of metal alkoxides (sol–gel transcription), by which one can control the morphology of inorganic compounds and generate various superstructural inorganic materials.[12] In a typical process of transcription that consists of several steps, LMWGs (templates) are brought into contact with inorganic precursor (e.g., metal alkoxide) in the gel phase. The deposition of inorganic precursor on the outer surface of the template will result in the formation of organic–inorganic hybrid material through electrostatic or hydrogen-bonding interactions between *anionic* oligomeric silica and the *cationic* LMWG fibers during the sol–gel polycondensation. Finally, the organic templates can be removed from the hybrid material either by washing with organic solvent or by heat treatment to obtain the superstructured inorganic material.

We have also introduced the templating concept to electrochemical polymerization process. Oxidative polymerization of monomers like aniline, pyrrole, ethylenedioxythiophene, etc. produces *cationic* intermediate that interacts through electrostatic attractive force with *anionic* assemblies of

Table 2. Schematic representation of various post-modification processes of the gel fibers

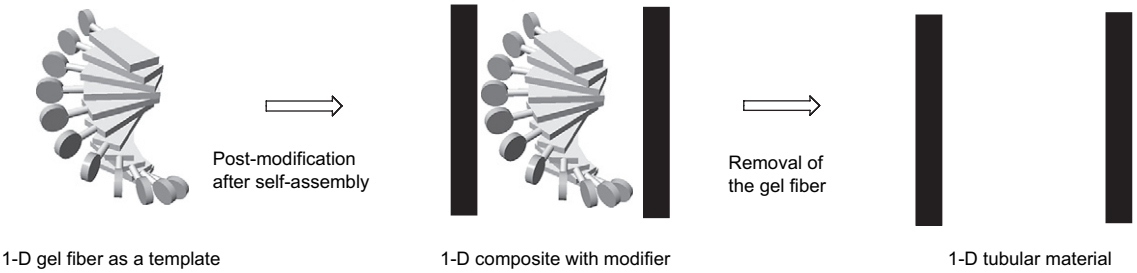

Template	Modifer
Cationic template	Anionic modifier (metal alkoxides such as SiO_2, TiO_2, etc.)
Anionic template	Cationic modifier (precursors of conductive polymers)
Neutral template (Ligand)	Neutral modifier (metal ions or complexes)

LMWG, acting as a potential template.[13] The template-based polymerization of monomers has provided the opportunity to create a novel kind of superstructure, which is generally unattainable from conventional polymerization process. These approaches are summarized in Table 2.

In the course of the above studies, it has occurred to us that post-modification of the gel fibers is also possible by means of *non-electrostatic interaction*, for example, by using metal–ligand interaction. Judging from the proposed aggregation mode (Fig. 2), this effect is particularly expected for **2** because a pyridyl nitrogen on **2** is perpendicularly oriented to the radius of the columnar aggregate and two nitrogen atoms in the neighboring pyridyl groups arranged along the helical staircase can face each other approximately in 180°. We therefore extensively investigated the influence of added metal ions (Ag(I), Pt(II), Cd(II), Co(II), Cu(II), Ni(II), Zn(II), Pd(II), etc.) on the gelation ability of **1**–**3** and found that a positive effect appeared in the combination of **2** and Ag(I). As shown in Figure 4, the T_{gel} values for **3** (10 g dm^{-3}) in diphenyl ether are less affected by added AgOTf. This is due to the poor coordination ability of the 2-pyridyl group. The T_{gel} values for **1** sharply lowered at low AgOTf concentration region and then flattened at around 80 °C. On the other hand, the sol solution of **2** in the presence of AgOTf is changed into the gel at [AgOTf]/[**2**]=0.02–0.06 and results in a precipitate above [AgOTf]/[**2**]=0.06. When the concentration of **2** is enhanced to 15 g dm^{-3}, the T_{gel} maximum appears at around [AgOTf]/[**2**]=0.05.

To obtain evidence for the Ag(I)–pyridine interaction in the gel phase we measured the ^{1}H NMR (600 MHz) spectra for gelatinous **2** (30 g dm^{-3} (59.2 mmol dm^{-3})) and **2**+AgOTf (11.8 mmol dm^{-3}) in benzene-d_6 at 25 °C. The particular difference between the two spectra is the down-field shift of the pyridyl 2-H from 8.141 ppm in the absence of AgOTf to 8.165 ppm in the presence of AgOTf. Also interesting is a morphological change induced by added AgOTf. In the absence of AgOTf, rod-like clusters are recognized. In the presence of AgOTf, on the other hand, fibrillar aggregates can be recognized. It is clear, therefore, that Ag(I) interacts with the 3-pyridyl nitrogens in **2** and changes the morphology into a fibrillar one, more suitable for gel formation.

The present study demonstrated that pyridine, which a priori shows versatile solubility in various solvents, is useful to design the versatile gelator based on the chlolesterol skeleton. Furthermore, their morphologies and gel stabilities can be modified by added Ag(I). We believe that further structural modifications (e.g., introduction of a spacer group between pyridine and cholesterol, quaternization of the pyridyl groups, etc.) will lead to further exploitation of these new functionalized gelators.

We then fabricated gel fibers with fluorescent molecule such as tetraphenyl porphyrin zinc(II) (ZnTPP) coordinated to the pyridine nitrogen atom. We therfore designed a new porphyrin modifier having photopolymerizable units at the end of the tether groups (**4**) (Fig. 5).

Firstly, we prepared a gel from **1** and **4**·**Zn**. Onto the 1-butyronitrile gel of **1** (17 mM) in a capped tube, a xylene solution of **4**·**Zn** (1.7 mM) was added. The mixture formed a bilayer of gel with porphyrin solution on top. After 6 h, the solution layer containing the porphyrin had diffused into the gel phase and the opaque gel turned violet. The UV–vis absorption spectral study of the colored gel (**1**+**4**·**Zn**) revealed that the Soret band of the porphyrin had shifted to longer wavelength (from 427 nm to 431 nm) concomitant with the bathochromic shift of the Q bands (561 nm to 565 nm and 603 nm to 606 nm) when compared with the homogeneous solution of **4**·**Zn** (Fig. 6a). The same study was conducted using **4**·**H**, which has no coordination

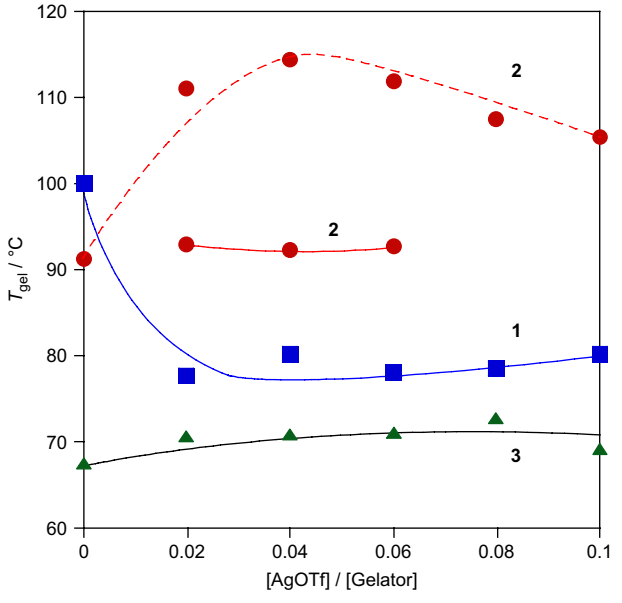

Figure 4. Plots of T_{gel} versus [AgOTf]/[**1**, **2**, or **3**] in diphenyl ether: [**1**, **2**, or **3**]=10 g dm^{-3} for the solid line, [**2**]=15 g dm^{-3} for the dotted line. In [**2**]=15 g dm^{-3}, the system became sol below [AgOTf]/[**2**]=0.02 whereas it became precipitate above [AgOTf]/[**2**]=0.06.

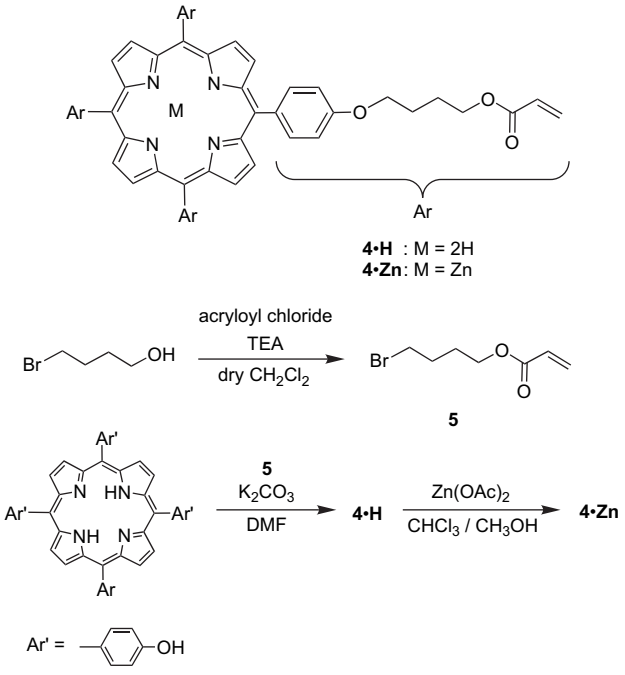

Figure 5. Chemical structure of **4**·**H** and **4**·**Zn** synthesized according to the above scheme.

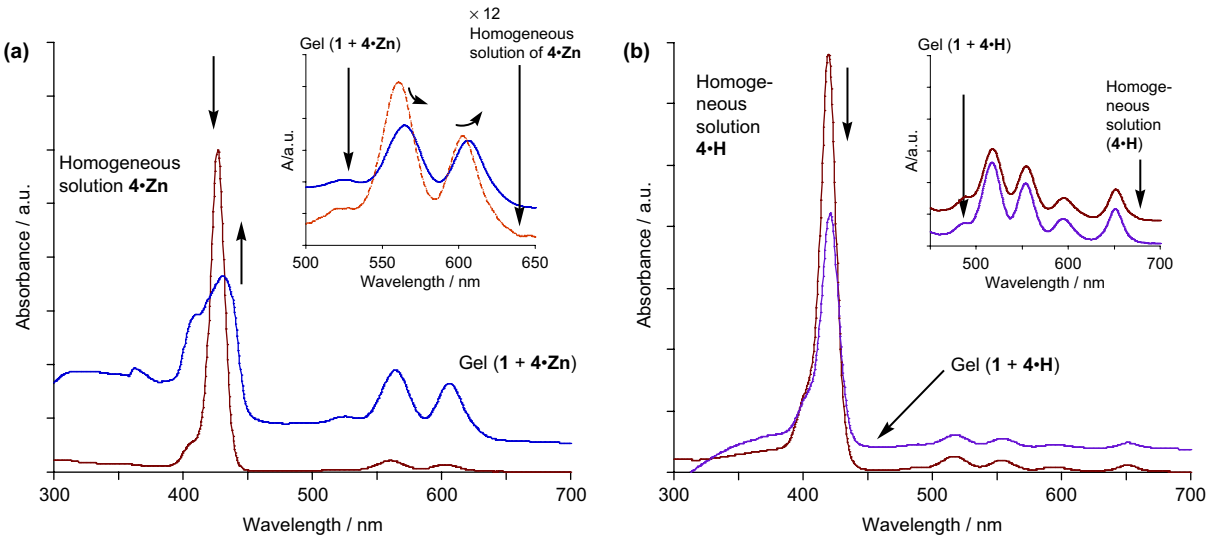

Figure 6. UV–vis absorption spectra of (a) **1**+**4**·**Zn** gel (butyronitrile) and **4**·**Zn** solution (xylene) and (b) **1**+**4**·**H** gel (butyronitrile) and **4**·**H** solution (xylene).

site on the porphyrin. Figure 6b clearly shows that neither any significant shifts of Soret band nor of the Q bands were observed. These spectral changes proved that pyridyl groups of **1** in the gel fibers interact with the zinc atoms in the porphyrin cores of **4**·**Zn** and the gel fibers are successfully decorated with the porphyrins at the surface.

To obtain direct images of fluorescent species in the gel fibers, we conducted confocal laser scanning microscopy (CLSM) observation. The sample was prepared using same conditions as in the UV–vis spectroscopy. In Figure 7a and b, entangled fibers colored with fluorescent dyes can clearly be seen for the sample prepared from **1** gel with **4**·**Zn**. As a contrast, the sample prepared from **1** gel with **4**·**H** did not show any fibrous morphology but instead showed small circular morphologies, which may come from particle aggregates of **4**·**H**. Given such results from TEM, UV–vis spectroscopy, and CLSM observations, we can conclude that the **4**·**Zn** molecules do indeed interact with the pyridyl groups of **1** accommodated in the gel fibers.

Finally, we conducted fixation of the porphyrins accumulated on the surface of the gel fibers by photopolymerization of the acryloyl moieties in **4**·**Zn**. Compound **1** (14 mM), **4**·**Zn** (1.4 mM), and 2,2-dimethoxy-2-phenylacetophenone (1.4 mM) as a photoinitiator were mixed in butyronitrile and the gel was prepared. After photoirradiation by a Xe lamp with monochromator (340 nm) for 8 h, the C=C stretching band of **4**·**Zn** at 1634 cm^{-1} observed by IR spectroscopy disappeared. This result indicates that most of the acryloyl moieties are consumed to form polymerized species. This should stabilize the porphyrin assemblies surrounding the gel fibers.

Chloroform is a good solvent for **1** and does not give rise to a one-dimensional superstructure of **1**. After the photopolymerization treatment of the **1** gel decorated with **4**·**Zn**, the sample was dispersed into chloroform and the solution was cast on a carbon-coated copper grid. The TEM image of this sample revealed that even after treatment with chloroform, the photopolymerized sample prepared from **4**·**Zn** and **1** still retains one-dimensional morphologies with cloudy contrast (Fig. 8a and b). This cloudy contrast perhaps comes from disassembled gelator **1**. From the TEM images, one can recognize that the one-dimensional structure partially forms a tubular structure (Fig. 8b, arrows). As shown in Figure 8, either the butyronitrile gel of **1** or the sample before rinsing treatment with chloroform after photopolymerization has similar one-dimensional morphologies with diameters ranging from 50 nm to 100 nm. These observations demonstrate that the polymerization of the zinc porphyrin (**4**·**Zn**) occurs along the **1** gel fibers and that the assembly is stabilized by the photopolymerization, resulting in the possible formation of porphyrin nanotubes.

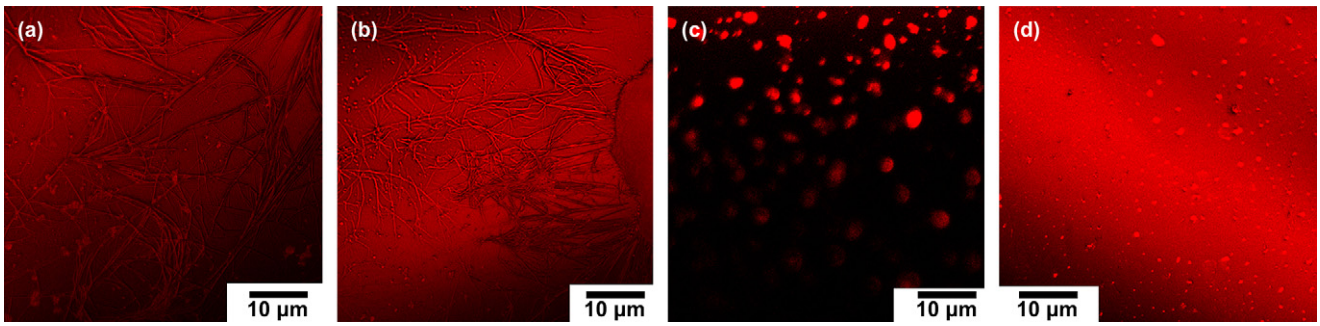

Figure 7. CLSM images of the composite gels of (a) and (b) **1**+**4**·**Zn** and (c) and (d) **1**+**4**·**H**.

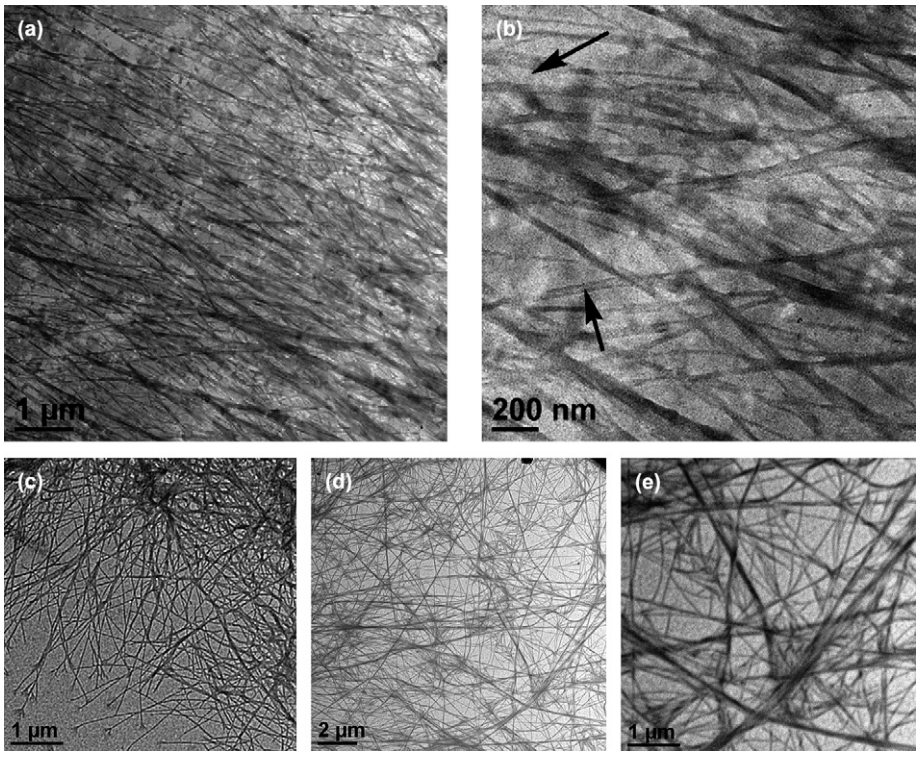

Figure 8. TEM images of the gel prepared from (a) and (b) **1**+**4**·**Zn** after photoirradiation and $CHCl_3$ rinsing, (c) **1**, and (d) and (e) **1**+**4**·**Zn** after photoirradiation before $CHCl_3$ rinsing.

3. Conclusions

In conclusion, the present study demonstrated that pyridine, which a priori has versatile solubility in various solvents, is useful to design a versatile gelator based on the chlolesterol skeleton. Even a solid solvent, naphthalene, can be stabilized. Furthermore, the morphologies and gel stabilities can be modified by added Ag(I). With Zn porphyrin (**4**·**Zn**), gelator **1** interacts through coordination and both the Soret band and Q bands are red shifted. CLSM observation, which is consistent with our expectation and shows the bright luminescent fibers, indicates that the fibers of **1** are decorated with zinc porphyrin (**4**·**Zn**). This is a unique example of fabrication of gel fiber and/or tubes with fluorescent molecules and this method of attaching fluorescent molecules to the gel fibers will provide novel applications in photochemical and electrochemical devices.

4. Experimental

4.1. General

Chemicals and solvents required were obtained from commercial suppliers and were used without further purification except for CH_2Cl_2 and diethyl ether, which are distilled over CaH_2 and sodium with benzophenone, respectively, before use. DMF was dried over CaH_2 for 8 h and distilled before use. Silica gel (40–50 μm) was purchased from KANTO. ^{1}H NMR spectra were measured on a Bruker AC-250PC and a Bruker DMX 600 apparatuses with tetramethylsilane as an internal standard. ATR FTIR spectra were recorded with a PerkinElmer Spectrum One. Mass spectral data were obtained using a Perseptive Voyager RP MALDI TOF mass spectrometer. TEM studies were carried out on a JEOL JEM-2010, operating at 120 kV. A Hitachi S-5000 scanning electron microscope was used for taking the SEM pictures at 25 kV. CLSM measurements were carried out at 543 nm excitation wavelength (He–Ne laser) using confocal laser scanning microscope (LSM-510, Carl Zeiss Co. Ltd.).

4.1.1. Synthesis.

4.1.1.1. Compound 1. To a dichloromethane (200 mL) solution of 4-aminopyridine (0.50 g, 5.3 mmol), triethylamine (3.0 mL, 22 mmol) was added under nitrogen and cooled in an ice bath. Into the solution, a dichloromethane solution (80 mL) of cholesteryl chloroformate (2.5 g, 5.6 mmol) was added dropwise over 1.5 h at 0 °C and the mixture was stirred for another day at room temperature. Chloroform was added to the reaction mixture and the solution was washed five times with HCl aq (0.1 M), twice with satd $NaHCO_3$ aq, and twice with H_2O and the organic layer was dried over Na_2SO_4. Chloroform was removed under reduced pressure to give **1** as white solid (2.6 g, 96%). Mp 192–193 °C; ^{1}H NMR (600 MHz, $CDCl_3$, 298 K, TMS) δ=0.68 (s, 3H), 0.86–0.87 (m, 6H), 0.92–2.44 (m, 34H), 4.60–4.66 (m, 1H), 5.41–5.42 (m, 1H), 6.74 (s, 1H), 7.32 (d, J=5.8 Hz, 2H), 8.46 (d, J=5.8 Hz, 2H). MS (MALDI-TOF, matrix; dithranol): calcd for [M+H$^+$] 507.39. Found 507.48. EA calcd for $C_{33}H_{50}BrN_2O_2$: C 78.21, H 9.94, N 5.53; found C 78.12, H 9.98, N 5.47. The same procedure was applied for the synthesis of **2** and **3**.

4.1.1.2. Compound 2. Compound **2** was obtained from 3-aminopyridine (0.50 g, 5.1 mmol) and cholesteryl chloroformate (2.5 g, 5.6 mmol) as white solid (0.81 g, 30%

yield). Mp 211–214 °C; ^{1}H NMR (600 MHz, $CDCl_3$, 298 K, TMS) δ=0.68 (s, 3H), 0.86 (m, 6H), 0.87–2.42 (m, 34H), 4.60–4.64 (m, 1H), 5.41 (s, 1H), 6.68 (s, 1H), 7.25 (t, J=4.7 Hz, 1H), 7.99 (s, 1H), 8.36 (d, J=4.4 Hz, 2H), 8.48 (s, 1H). MS (MALDI-TOF, matrix; dithranol): calcd for [M+H$^+$] 507.39. Found 507.48. EA calcd for $C_{33}H_{50}BrN_2O_2$: C 78.21, H 9.94, N 5.53; found C 78.26, H 9.95, N 5.54.

4.1.1.3. Compound 3. Compound **3** was obtained from 2-aminopyridine (1.54 g, 16.4 mmol) and cholesteryl chloroformate (4.9 g, 10.9 mmol) as white solid (2.0 g, 37% yield). Mp 199–200 °C; ^{1}H NMR (600 MHz, $CDCl_3$, 298 K, TMS) δ=0.69 (s, 3H), 0.86 (s, 6H), 0.87–2.43 (m, 34H), 4.61–4.65 (m, 1H), 5.41 (s, 1H), 6.97 (t, J=6.1 Hz, 1H), 7.67 (t, J=7.9 Hz, 1H), 7.71 (s, 1H), 7.96 (d, J=8.1 Hz, 1H), 8.25 (d, J=3.4 Hz, 1H). MS (MALDI-TOF, matrix; dithranol): calcd for [M+H$^+$] 507.39. Found 507.84. EA calcd for $C_{33}H_{50}BrN_2O_2$: C 78.21, H 9.94, N 5.53; found C 78.30, H 9.93, N 5.47.

4.1.1.4. Compound 5. To a CH_2Cl_2 (20 mL) solution of 4-bromo-1-butanol (3.8 mL, 40 mmol) and TEA (2.8 mL, 20 mmol), a CH_2Cl_2 (30 mL) solution of acryloyl chloride (3.6 mL, 44 mmol) was added dropwise and the reaction mixture was stirred at 0 °C to room temperature for 4 h. The solvent was removed under reduced pressure and the resultant residue was then subjected to column chromatography (SiO_2, $CHCl_3$/hexane=1:1) to give **5** as yellow oil (5.2 g, 64%). ^{1}H NMR (250 MHz, $CDCl_3$, 298 K, TMS) δ=1.80–2.03 (m, 4H), 3.45 (t, J=6.2 Hz, 2H), 4.18 (q, J=6.2 Hz, 2H), 5.83 (dd, J=10, 1.5 Hz, 1H), 6.11 (dd, J=17, 10 Hz, 1H), 6.40 (dd, J=17, 3.6 Hz, 1H).

4.1.1.5. Compound 4·H. A DMF (40 mL) solution of tetrakis(4-hydroxyphenyl)porphyrin (0.5 g, 0.74 mmol) and K_2CO_3 (2.0 g, 15 mmol) was stirred at 60 °C for 30 min. To the so1ution, **5** (3.0 g, 15 mmol) was added and the reaction mixture was stirred at 60 °C for 10 h. Ethyl acetate was added to the reaction mixture and the organic phase was washed twice with brine. After drying over Na_2SO_4, ethyl acetate was removed under reduced pressure and the residue was purified by recrystallization (CH_2Cl_2/hexane) to give **4·H** as a purple solid (0.77 g, 88%). ^{1}H NMR (600 MHz, $CDCl_3$, 298 K, TMS) δ=−2.75 (s, 2H), 2.04–2.06 (m, 16H), 4.27 (t, J=5.6 Hz, 8H), 4.37 (t, J=5.6 Hz, 8H), 5.87 (d, J=10 Hz, 4H), 6.20 (dd, J=17, 10 Hz, 4H), 6.47 (dd, J=17, 8.5 Hz, 4H), 7.25 (d, J=8.0 Hz, 8H), 8.10 (d, J=8.0 Hz, 8H), 8.86 (s, 8H). ^{13}C NMR (125 MHz, $CDCl_3$, 298 K, TMS) δ=25.616, 26.126, 64.307, 64.857, 67.545, 112.676, 119.750, 128.563, 130.751, 134.659, 135.607, 158.742, 166.342. IR-ATR (solid) ν_{max}: 3316, 3035, 2956, 2925, 2874, 1722, 1634, 1606, 1573, 1523, 1508, 1466, 1406, 1350, 1282, 1239, 1175, 1108, 1051, 979, 964, 839, 804, 790, 740, 713, 637, 629, 538. MS (FAB) calcd for M$^+$ 1182.4990, found 1182.5001.

4.1.1.6. Compound 4·Zn. To a $CHCl_3$ (40 mL) solution of **4·H** (0.6 g, 0.51 mmol), zinc(II) acetate dihydrate (0.56 g, 2.5 mmol) was added. The reaction mixture was stirred at room temperature for 2 h. The organic phase was washed three times with water and dried over Na_2SO_4. After removal of $CHCl_3$, the residue was purified by recrystallization (CH_2Cl_2/CH_3OH) to give **4·Zn** as a purple solid (0.60 g, 95%). ^{1}H NMR (600 MHz, $CDCl_3$, 298 K) δ=2.05–2.07 (m, 16H), 4.29 (t, J=5.0 Hz, 8H), 4.35 (t, J=6.0 Hz, 8H), 5.86 (d, J=10 Hz, 4H), 6.17 (dd, J=17, 10 Hz, 4H), 6.44 (d, J=17 Hz, 4H), 7.26 (d, J=8.0 Hz, 8H), 8.10 (d, J=8.0 Hz, 8H), 8.97 (s, 8H). IR-ATR (solid) ν_{max}: 3036, 2949, 2921, 2872, 1721, 1689, 1634, 1605, 1573, 1524, 1507, 1489, 1468, 1407, 1337, 1279, 1240, 1173, 1109, 1056, 994, 981, 967, 847, 797, 717, 641, 630, 541. ^{13}C NMR (125 MHz, $CDCl_3$, 298 K, TMS) δ=25.602, 26.125, 64.665, 67.528, 112.551, 120.764, 128.524, 130.739, 131.886, 132.050, 135.279, 135.407, 150.494, 158.573, 166.324. MS (FAB) calcd for M$^+$ 1244.4125, found 1244.4091.

Acknowledgements

We deeply thank Ms. Eri Okazaki and Prof. Fumito Tani for HRMS measurements. Financial support was provided by Grant-in-Aid (Nos. 15105004, 16750122, and 18033040) and 21st Century COE Project, Functional Innovation of Molecular Informatics from the MEXT and JSPS fellowship for S.M. and S.-i.K.

References and notes

1. Recent reviews: (a) Terech, P.; Weiss, R. G. *Chem. Rev.* **1997**, *97*, 3133–3159; (b) van Esch, J.; Schoonbeek, F.; de Loos, M.; Kooijman, H.; Veen, E. M.; Kellogg, R. M.; Feringa, B. L. *Supramolecular Science: Where It Is and Where It Is Going*; Ungaro, R., Dalcanale, E., Eds.; Kluwer: The Netherlands, 1999; p 233; (c) Shinkai, S.; Murata, K. *J. Mater. Chem.* **1998**, *8*, 485–495; (d) Gronwald, O.; Shinkai, S. *Chem.—Eur. J.* **2001**, *7*, 4329–4334; (e) *Low Molecular Mass Gelators*; Fages, F., Ed.; Topics in Current Chemistry 256; Springer: Berlin, Heidelberg, 2005; (f) *Molecular Gels*; Weiss, R. G., Terech, P., Eds.; Springer: The Netherlands, 2006; (g) George, M.; Weiss, R. G. *Acc. Chem. Res.* **2006**, *39*, 489–497; (h) Sugiyasu, K.; Fujita, N.; Shinkai, S. *J. Synth. Org. Chem. Jpn.* **2005**, *63*, 359–369.
2. (a) Bergeret-Galley, C.; Latouche, X.; Illouz, Y. G. *Aesthet. Plast. Surg.* **2001**, *25*, 249–255; (b) Duke, D.; Grevelink, J. M. *Dermatol. Surg.* **1998**, *24*, 201–206.
3. Jenning, V.; Gysler, A.; Schafer-Korting, M.; Gohla, S. H. *Eur. J. Pharm. Biopharm.* **2000**, *49*, 211–218.
4. Alvord, L.; Court, J.; Davis, T.; Morgan, C. F.; Schindhelm, K.; Vogt, J.; Winterton, L. *Optom. Vis. Sci.* **1998**, *75*, 30–36.
5. Kubo, W.; Murakoshi, K.; Kitamura, T.; Wada, Y.; Hanabusa, K.; Shirai, H.; Yanagida, S. *Chem. Lett.* **1998**, 1241–1242.
6. Ayabe, M.; Kishida, T.; Fujita, N.; Shinkai, S. *Org. Biomol. Chem.* **2003**, *1*, 2744–2747.
7. Sugiyasu, K.; Fujita, N.; Shinkai, S. *Angew. Chem., Int. Ed.* **2004**, *43*, 1229–1231.
8. (a) Suzuki, M.; Yumoto, M.; Kimura, K.; Shirai, H.; Hanabusa, K. *Chem. Commun.* **2002**, 704–705; (b) Kobayashi, H.; Friggeri, A.; Koumoto, K.; Amaike, M.; Shinkai, S.; Reinhoudt, D. N. *Org. Lett.* **2002**, *4*, 1423–1424; (c) Luboradzki, R.; Gronwald, O.; Ikeda, A.; Shinkai, S. *Chem. Lett.* **2002**, 1148–1149.
9. Snip, E.; Shinkai, S.; Reinhoudt, D. N. *Tetrahedron Lett.* **2001**, *42*, 2153–2156.
10. (a) van Bommel, K. J. C.; Shinkai, S. *Langmuir* **2002**, *18*, 4544–4548; (b) Kawano, S.-i.; Fujita, N.; van Bommel, K. J. C.; Shinkai, S. *Chem. Lett.* **2003**, *32*, 12–13.

11. (a) Malik, S.; Rochas, C.; Guenet, J. M. *Macromolecules* **2005**, *38*, 4888–4893; (b) Dasgupta, D.; Manna, S.; Malik, S.; Rochas, C.; Guenet, J. M.; Nandi, A. K. *Macromolecules* **2005**, *38*, 5602–5608; (c) Malik, S.; Roizard, D.; Guenet, J. M. *Macromolecules* **2006**, *39*, 5957–5959.
12. (a) Estroff, L. A.; Hamilton, A. D. *Chem. Mater.* **2001**, *13*, 3227–3235; (b) Davis, S. A.; Breulmann, M.; Rhodes, K. H.; Zhang, B.; Mann, S. *Chem. Mater.* **2001**, *13*, 3218–3226; (c) van Bommel, K. J. C.; Friggeri, A.; Shinkai, S. *Angew. Chem., Int. Ed.* **2003**, *42*, 980–999; (d) Sone, E. D.; Zubarev, E. R.; Stupp, S. I. *Angew. Chem., Int. Ed.* **2002**, *41*, 1706–1709; (e) Sone, E. D.; Zubarev, E. R.; Stupp, S. I. *Small* **2005**, *1*, 694–697; (f) Smith, D. K. *Adv. Mater.* **2006**, *18*, 2773–2778; (g) Kim, C.; Lee, S. J.; Lee, I. H.; Kim, K. T.; Song, H. H.; Jeon, H.-J. *Chem. Mater.* **2003**, *15*, 3638–3642; (h) Ono, Y.; Nakashima, K.; Sano, M.; Kanekiyo, Y.; Inoue, K.; Hojo, J.; Shinkai, S. *Chem. Commun.* **1998**, 1477–1478; (i) Jung, J. W.; Ono, Y.; Sakurai, K.; Sano, M.; Shinkai, S. *J. Am. Chem. Soc.* **2000**, *122*, 8648–8653; (j) Jung, J. W.; Ono, Y.; Shinkai, S. *Angew. Chem.* **2000**, *39*, 1862–1863; (k) Kawano, S.-i.; Fujita, N.; Shinkai, S. *Chem.—Eur. J.* **2004**, *10*, 343–351; (l) Tamaru, S.-i.; Takeuchi, M.; Sano, M.; Shinkai, S. *Angew. Chem., Int. Ed.* **2002**, *41*, 853–856.
13. (a) Hatano, T.; Bae, A.-H.; Takeuchi, M.; Fujita, N.; Kaneko, K.; Ihara, H.; Takafuji, M.; Shinkai, S. *Chem.—Eur. J.* **2004**, *10*, 5067–5075; (b) Li, C.; Hatano, T.; Takeuchi, M.; Shinkai, S. *Chem. Commun.* **2004**, 2350–2351.